Since January 2020 Elsevier has created a COVID-19 resource centre with free information in English and Mandarin on the novel coronavirus COVID-19. The COVID-19 resource centre is hosted on Elsevier Connect, the company's public news and information website.

Virology 435 (2013) 210–213

Contents lists available at SciVerse ScienceDirect

Virology

journal homepage: www.elsevier.com/locate/yviro

Rapid Communication

Murine hepatitis virus nsp4 N258T mutants are not temperature-sensitive

Dia C. Beachboard [a], Xiaotao Lu [b], Susan C. Baker [c], Mark R. Denison [a,b,*]

[a] Department of Pathology, Microbiology and Immunology, Vanderbilt University Medical Center, 1161 21st Avenue South, Nashville, TN 37232, USA
[b] Department of Pediatrics, Vanderbilt University Medical Center, 1161 21st Avenue South, Nashville, TN 37232, USA
[c] Department of Microbiology and Immunology, Loyola University Chicago Stritch School of Medicine, 2160 South First Avenue, Maywood, IL 60153, USA

ARTICLE INFO

Article history:
Received 13 August 2012
Returned to author for revisions
15 September 2012
Accepted 1 October 2012
Available online 23 October 2012

Keywords:
Coronavirus
Murine hepatitis virus
Replication
Non-structural protein 4
nsp4
Temperature-sensitive mutants
Cell biology

ABSTRACT

Coronavirus replicase nsp4 is critical for virus-induced membrane modifications. An nsp4 mutant (N258T) of murine hepatitis virus (MHV) has been reported to be temperature-sensitive (ts) and to alter membrane targeting. We engineered and recovered all four possible codon variants of N258T in the cloned MHV-A59 background. All mutant viruses demonstrated impaired replication compared to wildtype MHV, but no nsp4 N258T mutant virus was ts, and all variants colocalized with viral protein markers for replication complexes, but not with markers for mitochondria. This study emphasizes that complete genome sequencing may be necessary, even with directed and confirmed reverse genetic mutants.

The study

Coronaviruses, like other RNA viruses, induce modifications of cytoplasmic membranes in order to form replication complexes, as sites of viral RNA synthesis. Three of the coronavirus-encoded replicase non-structural proteins, nsps3, 4 and 6, contain membrane-spanning domains and are thought to be essential for cytoplasmic membrane modifications (Baliji et al., 2009; Imbert et al., 2008; Kanjanahaluethai et al., 2007; Oostra et al., 2008). The topology of nsp4 in membranes has been described and nsp4 has been shown to localize to replication complexes (Gadlage et al., 2010; Hagemeijer et al., 2011; Oostra et al., 2007). Mutations in nsp4 of murine hepatitis virus (MHV) decrease viral RNA synthesis and viral growth, and modification of glycosylation sites within the first luminal loop of nsp4, alters the electron micrograph morphology of virus-induced double-membrane vesicles (DMVs) (Gadlage et al., 2010; Sparks et al., 2007).

Sawicki et al. analyzed a known temperature-sensitive(ts) mutant of MHV, Alb ts6, by sequence and reversion analysis. They identified within the nsp4 coding region an A$\underline{A}_{9494}$T-to-A$\underline{C}_{9494}$T nucleotide (nt) change resulting in an Asn258Thr (N258T) substitution as the putative ts mutation (Sawicki et al., 2005; Sturman et al., 1987). Clementz et al. engineered the N258T substitution in recombinant MHV using a two nt change A$\underline{AT}_{9494–9495}$-to-A$\underline{CA}_{9494–9495}$. The resulting virus, Alb ts6 icv, was reported to be ts at 39.5 °C, and to demonstrate altered distribution of nsp4 in the infected cell, colocalizing with protein markers for the mitochondria. It was concluded that nsp4, and particularly residue N258, is important for membrane localization (Clementz et al., 2008). Subsequently, Sparks et al. (2008) sequenced an Alb ts6 isolate and found four non-synonymous mutations in the complete genome sequence that did not include the previously reported N258T substitution, but instead identified a Val148Ala (V148A) substitution in nsp5 (3CLpro), which was ultimately confirmed by reverse genetics and complete genome sequencing to be responsible for the ts phenotype.

We sought to reconcile these disparate results, using our established reverse genetic system (Yount et al., 2002) to engineer N258T$_{ACA}$ into the same wildtype (WT)-MHV-A59 isogenic background as reported by Clementz et al. (2008). The introduced mutations would require a two nt change for primary reversion to Asn (Fig. 1). The N258T$_{ACA}$ virus was recovered at 30 °C and two rounds of plaque purification were performed prior to expansion and determination of the genome sequence from nt 10 to 31334 by the di-deoxy (Sanger) approach. The A$\underline{AT}$ to A$\underline{CA}$ change was confirmed and no other changes from the cloned isogenic genome sequence were identified. In order to measure temperature sensitivity, efficiency of plating (EOP) is calculated as the titer at the non-

* Corresponding author at: Department of Pediatrics, Vanderbilt University Medical Center, D6217 MCN, 1161 21st Avenue South, Nashville, TN 37232-2581, USA. Fax: +1 615 343 9723.
E-mail address: mark.denison@vanderbilt.edu (M.R. Denison).

0042-6822/$ - see front matter © 2012 Elsevier Inc. All rights reserved.
http://dx.doi.org/10.1016/j.virol.2012.10.001

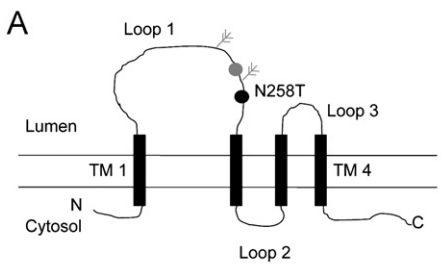

B

Virus	Titer at: 30°C	Titer at: 40°C	EOP (40/30)
WT N258$_{AAT}$	1.2 x 10^9	9.3 x 10^8	0.79
[1]N258T$_{ACA}$	5.4 x 10^7	2.8 x 10^7	0.52
N258T$_{ACC}$	4.6 x 10^7	3.5 x 10^7	0.77
N258T$_{ACG}$	4.3x 10^7	3.7 x 10^7	0.88
[2]N258T$_{ACT}$	1.2 x 10^7	2.3 x 10^7	2.10
V148A	1.3 x 10^8	1.9 x 10^3	1.4 x 10^{-5}

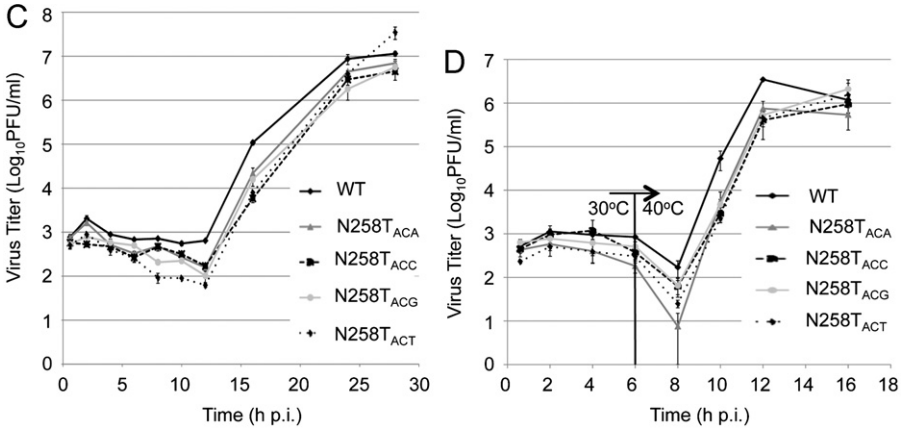

Fig. 1. Analysis of nsp4 N258T codon variant mutants of MHV. (A) Proposed topology of MHV nsp4: nsp4 has 4 membrane-spanning regions (TM1–4, black rectangles) and three loop regions (loop 1–3). Previously reported mutations in loop 1 are indicated as the gray double-headed arrows (glycosylation sites) and a gray dot (E226A/E227A) (Gadlage et al., 2010; Sparks et al., 2007). The N258T (AAT to ACX at nt positions 9493–9495) substitution is shown as a black dot. (B) Titers were determined by plaque assay in DBT cells at 30 °C and 40 °C. EOP was calculated as the titer at 40 °C divided by the titer at 30 °C. Titers represent the average titer of two independent experiments. [1] Codon variant previously reported by Clementz et al. (2008), [2] Codon variant previously reported by Sawicki et al. (2005). (C) DBT cells were infected at an MOI of 0.1 PFU/cell with the indicated viruses and incubated at 30 °C for 28 h and titers were determined by plaque assay. Error bars represent the standard error of the mean of two independent plaque assays done in duplicate. (D) DBT cells were infected at an MOI of 0.1 PFU/cell with the indicated viruses and incubated at 30 °C with a temperature shift to 40 °C at 6 h p.i. and titers were determined by plaque assay. Error bars represent the standard error of the mean of two independent plaque assays done in duplicate.

permissive temperature (40 °C) divided by the titer at the permissive temperature (30 °C). When WT and N258T$_{ACA}$ viruses were compared for EOP, N258T$_{ACA}$ demonstrated an EOP similar to WT, and without a ts phenotype (Fig. 1).

The finding that N258T$_{ACA}$ was not ts by EOP lead us to the questions: why our engineered mutant virus was different than the one reported by Clementz et al.; whether there were additional changes in their virus that led to the observed phenotypes; and if the phenotype was codon-specific . Therefore, we engineered viruses containing the T$_{ACC}$, T$_{ACG}$ and T$_{ACT}$ codon variants. All three Thr258 codon variant viruses, N258T$_{ACA}$, N258T$_{ACC}$, and N258T$_{ACT}$, were recovered at 30 °C. Sanger sequencing of the complete nsp4 domain confirmed the introduced mutations and no additional mutations were identified.

All codon variant N258T viruses were tested for temperature-sensitivity by plaque assay in murine DBT cells at the permissive (30 °C) and non-permissive (40 °C) temperatures and EOP was calculated (Fig. 1). WT virus had an EOP of 0.79 demonstrating that there is no growth impairment at 40 °C. As a ts control, the EOP of nsp5 tsV148A, was performed in parallel and calculated to be 1.4×10^{-5}, confirming the ts phenotype. All four codon variant viruses had WT-like EOPs (0.52–2.10) indicating that they are not impaired for growth at 40 °C, inconsistent with a ts phenotype (Fig. 1). Because plaque growth and numbers are only a measure of fitness and temperature sensitivity, we next compared growth of the mutant viruses at 30 °C. DBT cells were infected at an MOI of 0.1 PFU/cell and supernatant was sampled at 0.6, 2, 4, 6, 8, 10, 12, 16, 24, and 28 h p.i. for plaque assay (Fig. 1). At 30 °C, all four codon mutants had indistinguishable growth characteristics and achieved peak titers similar to WT at 28 h p.i. However, between 8 and 24 h p.i., the codon mutant viruses exhibited a lag in exponential growth with a 0.5 to 1 log 10 decrease in viral titers during this phase, consistent with a stable replication defect and likely decreased fitness compared with WT (Fig. 1).

We then tested growth following a temperature shift from 30 °C to 40 °C at 6 h p.i., with supernatants sampled at 0.6, 2, 4, 6, 8, 10, 12, and 16 h p.i. WT virus growth kinetics demonstrated an initial decrease in titer immediately following the temperature shift, but recovered quickly, and achieved peak titers by 12 h p.i. All four codon mutants grew indistinguishably from each other, and achieved WT-like peak titers at 16 h p.i. Similar to growth at 30 °C, between 8 and 16 h p.i., the codon mutants exhibited a lag in exponential growth and decreased viral titers compared to WT (Fig. 1). These data demonstrate that while the N258T substitution within nsp4 exhibited impairment in growth, it did not confer temperature-sensitivity, contrary to what has been previously reported.

The N258T$_{ACA}$ virus reported by Clementz et al. (2008). was concluded to have altered localization of nsp4 to mitochondrial membranes at 39.5 °C. To determine the localization of our mutant nsp4 proteins, DBT cells were infected with WT, N258T$_{ACA}$, N258T$_{ACC}$, N258T$_{ACG}$, and N258T$_{ACT}$ on glass coverslips at an MOI of 5 PFU/cell for 16 h at 30 °C or for 7 h at 40 °C (Fig. 2). Infected cells were then fixed and permeabilized with methanol, immunostained with antibodies specific to nsp4 and nsp8 or pyruvate dehydrogenase (PDH), a mitochondrial matrix protein. Cells were imaged using a Zeiss LSM510 confocal microscope.

At both 30 °C and 40 °C, for WT and all N258T codon substitutions, nsp4 and nsp8 extensively colocalized to punctate perinuclear foci (Fig. 2 and data not shown). In contrast, both WT and

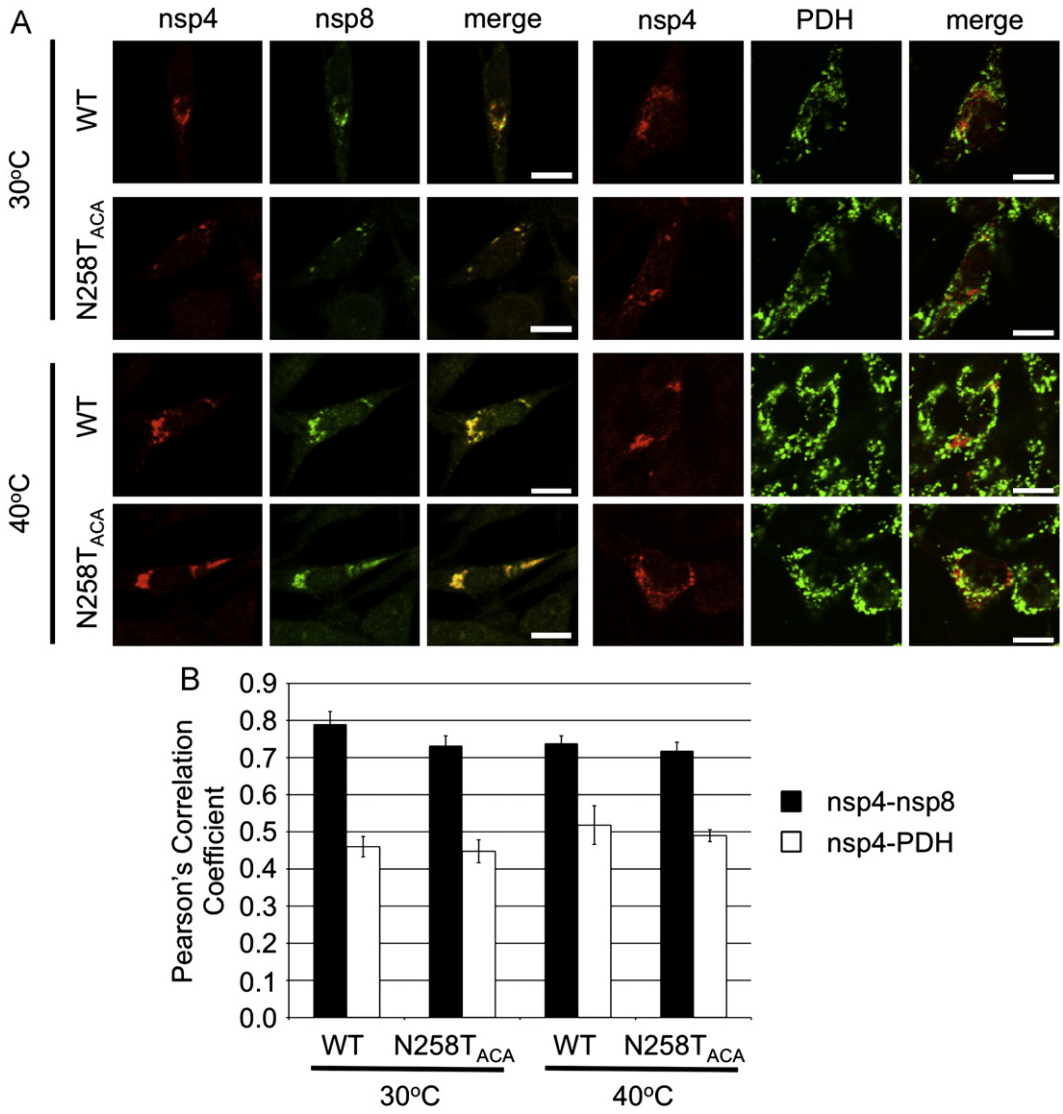

Fig. 2. (A) Nsp4 N258T$_{ACA}$ codon variant localizes to the replication complex. DBT cells were infected at an MOI of 5 PFU/cell for 16 h at 30 °C or 7 h at 40 °C. Cells were fixed in methanol, probed for nsp4 (red) and nsp8 (green) or PDH (green) and imaged on a Zeiss LSM510 confocal microscope. Yellow pixels represent colocalization of overlapping red and green pixels. The scale bar in the bottom right corner of merged images represents 10 μm. (B) Pearson's correlation coefficient was calculated for nsp4-nsp8 or nsp4-PDH for both WT and N258T$_{ACA}$ at 30 °C and 40 °C ($n=5$). Error bars represent standard deviation.

mutant viruses display non-colocalization of nsp4 and PDH. Nsp4 localized to punctate perinuclear foci, whereas PDH localized to foci dispersed throughout the cytoplasm that were adjacent to but distinct from nsp4 foci. Within the same fields of view, there were infected cells that had not formed syncytia as well as syncytial cells and the pattern of colocalization were consistent between both sets of infected cells as well as within a z-stack . In order to quantify colocalization, Pearson's correlation coefficient was calculated using the JACoP plugin for ImageJ (Bolte and Cordelieres, 2006; Schneider et al., 2012). To avoid bias, colocalization was quantified for the entire field and the entire z-stack of five images per condition. At both 30 °C and 40 °C, WT and N258T$_{ACA}$ nsp4 and nsp8 had Pearson's correlation coefficients of between 0.71 and 0.79, respectively, consistent with colocalization. Nsp4 and PDH displayed Pearson's correlation coefficients of 0.45 to 0.52 ($p<.002$), respectively, demonstrating non-colocalization (Fig. 2). These results demonstrate that the nsp4 N258T substitution did not result in altered localization of nsp4 to the mitochondria at either 30 °C or 40 °C.

Conclusions

Our results demonstrate that the nsp4 N258T substitution is not responsible for either the ts phenotype, or for the altered localization of nsp4 to the mitochondria reported by Clementz et al. Although the nsp4 N258T codon variant viruses were not ts, they displayed decreased titers and delayed growth, demonstrating that N258 or loop 1 of nsp4 is likely important for replication. Interestingly, this residue is highly conserved among beta-coronaviruses, including bovine coronavirus, human coronavirus OC43 and SARS-CoV as an aspartic acid, with MHV being the exception. The conservation of this residue suggests that it may be important. Our lab has previously reported two nsp4 mutant viruses, with mutations located in luminal loop 1. Nsp4 contains two glycosylation sites at N176 and N237 (Fig. 1), that when substituted with alanine, demonstrate delayed growth and decreased viral titers similar to those of nsp4 N258T, as well as altered DMV formation (Gadlage et al., 2010). The nsp4 E226A/E227A mutant virus (Fig. 1) is debilitated for growth and viral RNA synthesis (Sparks et al.,

2007). Together, these mutations suggest that loop 1 of nsp4 is important for viral replication, RNA synthesis, and formation of DMVs.

We are unable to explain the results reported by Clementz et al. because the virus was not available for direct comparison. However, our EOP results were confirmed by the Baker lab (data not shown). The reverse genetics system uses seven cDNA fragments that are ligated for transcription of genomic RNA that is then electroporated into cells for virus recovery. There is the possibility that mutations arose during amplification or transcription of the cloned fragments. Our lab and the Baker lab have the same original source for the cDNA fragments. In order to account for changes during amplification, we obtained all seven cDNA fragments from the Baker lab and attempts to recover virus were unsuccessful. We sequenced the cDNA fragment containing nsp4 and identified the $N258T_{ACA}$ substitution, as well as a single nucleotide deletion at nt 8582 that resulted in a possible stop codon (UGA at nt 8644 to 8646). The virus reported by Clementz et al. was difficult to recover (personal communication), leading to the possibility of multiple adaptive changes. The virus was not available for sequencing; therefore, we could not test for additional mutations. The experiments in this study were performed in MHV-A59, and it is important to consider polymorphisms within different strains of virus when analyzing the importance of specific residues. The results of our study strongly suggest that sequencing of the entire genome of mutant coronaviruses derived from the reverse genetics approach may be necessary. Several studies have documented mutations that arise during the process of mutagenesis or propagation of cDNA clones, as well as adaptive mutations that may occur in genes not thought to have any relationship. We demonstrated that the original MHV infectious clone had WT-like replication in culture, but was attenuated in vivo (Sperry et al., 2005). Complete genome sequencing found mutations in other fragments that arose during propagation of the clones that were confirmed to be responsible for the attenuating phenotype. Hurst et al. (2010) showed that impairment in MHV replication by mutations in the nucleocapsid gene resulted in compensating second-site mutations in the replicase protein nsp3. Thus coronaviruses may have unexpected linked functions or epistatic relationships that might be missed by partial sequencing. Fortunately, the cost and time of genome sequencing is rapidly improving. Establishment and availability of validated primer sets may allow for more rapid sequencing in a 96 well format or by deep sequencing, further reducing the cost and time associated with complete genome analysis, and may identify novel and important new relationships among coronavirus proteins.

Acknowledgments

This work was supported by Public Health Service award RO1 AI50083 (M.R.D.) from the National Institute of Allergy and Infectious Disease. D.C.B. was supported by Immunobiology of Blood and Vascular Systems through the Vanderbilt University School of Medecine (T32HL697659). This work was also supported by the Elizabeth B. Lamb Center for Pediatric Research.

References

Baliji, S., Cammer, S.A., Sobral, B., Baker, S.C., 2009. Detection of nonstructural protein 6 in murine coronavirus-infected cells and analysis of the transmembrane topology by using bioinformatics and molecular approaches. J. Virol. 83, 6957–6962.

Bolte, S., Cordelieres, F.P., 2006. A guided tour into subcellular colocalization analysis in light microscopy. J. Microsc. 224, 213–232.

Clementz, M.A., Kanjanahaluethai, A., O'Brien, T.E., Baker, S.C., 2008. Mutation in murine coronavirus replication protein nsp4 alters assembly of double membrane vesicles. Virology 375, 118–129.

Gadlage, M.J., Sparks, J.S., Beachboard, D.C., Cox, R.G., Doyle, J.D., Stobart, C.C., Denison, M.R., 2010. Murine hepatitis virus nonstructural protein 4 regulates virus-induced membrane modifications and replication complex function. J. Virol. 84, 280–290.

Hagemeijer, M.C., Ulasli, M., Vonk, A., Reggiori, F., Rottier, P.J., de Haan, C.A., 2011. Mobility and interactions of the coronavirus nonstructural protein 4. J. Virol. 85, 4572–4577.

Hurst, K.R., Ye, R., Goebel, S.J., Jayaraman, P., Masters, P.S., 2010. An interaction between the nucleocapsid protein and a component of the replicase–transcriptase complex is crucial for the infectivity of coronavirus genomic RNA. J. Virol. 84, 10276–10288.

Imbert, I., Snijder, E.J., Dimitrova, M., Guillemot, J.C., Lecine, P., Canard, B., 2008. The SARS-Coronavirus PLnc domain of nsp3 as a replication/transcription scaffolding protein. Virus Res. 133, 136–148.

Kanjanahaluethai, A., Chen, Z., Jukneliene, D., Baker, S.C., 2007. Membrane topology of murine coronavirus replicase nonstructural protein 3. Virology 361, 391–401.

Oostra, M., Hagemeijer, M.C., van Gent, M., Bekker, C.P., te Lintelo, E.G., Rottier, P.J., de Haan, C.A., 2008. Topology and membrane anchoring of the coronavirus replication complex: not all hydrophobic domains of nsp3 and nsp6 are membrane spanning. J. Virol. 82, 12392–12405.

Oostra, M., te Lintelo, E.G., Deijs, M., Verheije, M.H., Rottier, P.J., de Haan, C.A., 2007. Localization and membrane topology of coronavirus nonstructural protein 4: involvement of the early secretory pathway in replication. J. Virol. 81, 12323–12336.

Sawicki, S.G., Sawicki, D.L., Younker, D., Meyer, Y., Thiel, V., Stokes, H., Siddell, S.G., 2005. Functional and genetic analysis of coronavirus replicase–transcriptase proteins. PLoS Pathog. 1, e39.

Schneider, C.A., Rasband, W.S., Eliceiri, K.W., 2012. NIH image to imageJ: 25 years of image analysis. Nat. methods 9, 671–675.

Sparks, J.S., Donaldson, E.F., Lu, X., Baric, R.S., Denison, M.R., 2008. A novel mutation in murine hepatitis virus nsp5, the viral 3C-like proteinase, causes temperature-sensitive defects in viral growth and protein processing. J. Virol. 82, 5999–6008.

Sparks, J.S., Lu, X., Denison, M.R., 2007. Genetic analysis of Murine hepatitis virus nsp4 in virus replication. J. Virol. 81, 12554–12563.

Sperry, S.M., Kazi, L., Graham, R.L., Baric, R.S., Weiss, S.R., Denison, M.R., 2005. Single-amino-acid substitutions in open reading frame (ORF) 1b-nsp14 and ORF 2a proteins of the coronavirus mouse hepatitis virus are attenuating in mice. J. Virol. 79, 3391–3400.

Sturman, L.S., Eastwood, C., Frana, M.F., Duchala, C., Baker, F., Ricard, C.S., Sawicki, S.G., Holmes, K.V., 1987. Temperature-sensitive mutants of MHV-A59. Adv. Exp. Med. Biol. 218, 159–168.

Yount, B., Denison, M.R., Weiss, S.R., Baric, R.S., 2002. Systematic assembly of a full-length infectious cDNA of mouse hepatitis virus strain A59. J. Virol. 76, 11065–11078.